(*cf.* Gradshteyn & Ryzhik, 1980, entry 6.684.1), we arrive at the expression given for this coefficient in Table 1.

References

ABRAMOWITZ, M. & STEGUN, I. (1972). *Handbook of Mathematical Functions.* New York: Dover.
BARAKAT, R. (1974). *Optica Acta,* **21,** 903–921.
BERG, P. W. & MCGREGOR, J. L. (1966). *Elementary Partial Differential Equations.* San Francisco: Holden-Day.
DAVIS, P. J. & RABINOVITZ, P. (1967). *Numerical Integration.* London: Blaisdell.
GRADSHTEYN, I. S. & RYZHIK, I. M. (1980). *Tables of Integrals, Series and Products.* New York: Academic Press.
KENDALL, M. G. & STUART, A. (1969). *The Advanced Theory of Statistics,* Vol. 1, 3rd ed. London: Charles Griffin.
SHMUELI, U. (1979). *Acta Cryst.* A**35,** 282–286.
SHMUELI, U. (1982*a*). *Acta Cryst.* A**38,** 362–371.
SHMUELI, U. (1982*b*). In *Crystallographic Statistics: Progress and Problems,* edited by S. RAMASESHAN, M. F. RICHARDSON & A. J. C. WILSON, pp. 53–82. Bangalore: Indian Academy of Sciences.
SHMUELI, U. & KALDOR, U. (1981). *Acta Cryst.* A**37,** 76–80.
SHMUELI, U. & KALDOR, U. (1983). *Acta Cryst.* A**39,** 619–621.
SHMUELI, U. & WEISS, G. H. (1985). *Acta Cryst.* A**41,** 401–408.
SHMUELI, U., WEISS, G. H. & KIEFER, J. E. (1985). *Acta Cryst.* A**41,** 55–59.
SHMUELI, U., WEISS, G. H., KIEFER, J. E. & WILSON, A. J. C. (1984). *Acta Cryst.* A**40,** 651–660.
SHMUELI, U. & WILSON, A. J. C. (1981). *Acta Cryst.* A**37,** 342–353.
SHMUELI, U. & WILSON, A. J. C. (1983). *Acta Cryst.* A**39,** 225–233.
SPIEGEL, M. R. (1974). *Fourier Analysis.* Schaum's Outline Series. New York: McGraw-Hill.
WEISS, G. H., SHMUELI, U., KIEFER, J. E. & WILSON, A. J. C. (1985). In *Structure and Statistics in Crystallography,* edited by A. J. C. WILSON, pp. 23–42. Guilderland (NY): Adenine Press.
WILSON, A. J. C. (1949). *Acta Cryst.* **2,** 318–321.

The Effect of Ionic Deformation on One-Phonon X-ray Scattering

BY JOHN S. REID

Department of Physics, Natural Philosophy Building, University of Aberdeen, Aberdeen AB9 2UE, Scotland

Abstract

Explicitly representing the deformation of ions by the lattice dynamical shell model, the one-phonon scattering is written in a form that is amenable to direct evaluation. An analytic expression for the shell scattering factor is introduced, and the percentage alteration in the scattering brought about by the ionic deformation during vibration is calculated. Contour plots of the effect are presented for GaAs, ZnS and Si as representative of the zinc-blende-structure compounds and group IV elements. The alteration produced by shell models is found to be negative, because for these materials the shell moves less than the core. Its maximum value varies from about $-2 \cdot 5$ to -15% depending on the material and lattice dynamical model used. Its structure in reciprocal space should be measurable and could lead to a better understanding of deformation processes.

Introduction

Continuing interest on how the deformation of an ion during vibration affects the scattering factors led to an earlier study by Reid (1983*b*) on the modification of the Debye–Waller factor likely to arise from this process. Using different shell models to represent the deforming ions, a quantitative analysis was made for 14 zinc-blende-structure materials.

Since then, Matthew & Yousif (1984) have highlighted the quantum-mechanical justification inherent in the shell model approach. It is therefore natural to complete the enquiry by asking what quantitative effects are expected from such deformation processes on one-phonon (X-ray) scattering. This scattering is of course not confined to Bragg reflections and therefore gives a better picture of the decay of the effect with increasing scattering vector than is provided by the Debye–Waller factors.

The additional scattering processes

Earlier studies of the effect of deforming atoms [*e.g.* Melvin, Pirie & Smith (1968); Reid (1974); March & Wilkins (1978)] followed the lead of Born (1942) by introducing deformation parameters $\beta(ll', kk', \mathbf{K})$ that described the dependence of the scattering factor for the atom (lk) on the motion of the atom $(l'k')$ for scattering vector $\mathbf{K}$. With a particular model of the deforming atom, such as the archetypal shell model, this approach is distracting and unnecessary. The usual one-phonon scattering cross section may be written in electron units per cell as

$$I(\mathbf{K})/N\sigma_0 I_0 = \sum_j (E/\omega^2)_{\mathbf{q}j} | \sum_k f_k(K) \exp(-W_k)$$

$$\times \mathbf{K} . \mathscr{E}(k/\mathbf{q}j)/m_k^{1/2} \exp[i\mathbf{G} . \mathbf{r}(k)]|^2$$

$$\times \Delta(\mathbf{K}+\mathbf{q}, \mathbf{G}) \tag{1}$$

in one version of a commonly used notation (see Appendix).

Following the earlier approach of Reid (1983b) of considering each ion k to be represented by a core and a shell, and introducing the conventional relative shell–core displacement eigenvector $\mathscr{W}(k/\mathbf{q}j)$, as defined for example by Cochran & Cowley (1967), leads directly to a modified one-phonon scattering $I_s(\mathbf{K})$, where

$$I_s(\mathbf{K})/N\sigma_0 I_0 = \sum_j (E/\omega^2)_{\mathbf{q}j} |\sum_k f_k(K) \exp(-W_k)$$

$$\times \mathbf{K} . \mathscr{E}(k/\mathbf{q}j)/m_k^{1/2} \exp[i\mathbf{G} . \mathbf{r}(k)]$$

$$+ f_{sk}(K) \exp(-W_k)\mathbf{K} . \mathscr{W}(k/\mathbf{q}j)$$

$$\times \exp[i\mathbf{G} . \mathbf{r}(k)]|^2 \Delta(\mathbf{K}+\mathbf{q}, \mathbf{G}). \quad (2)$$

The effect of the ionic deformation is therefore to give rise to extra scattering processes, coherent with the normal processes, that may add or subtract intensity depending on the relation of $\mathscr{W}(k/\mathbf{q}j)$ to the core displacement eigenvector $\mathscr{E}(k/\mathbf{q}j)/m_k^{1/2}$. $f_{sk}(K)$ is the scattering factor of the shell of the kth ion, taken in the spirit of the shell model as dependent on the magnitude of $\mathbf{K}$. The only other developmental approximation made in (2) has been to take the Debye–Waller term $\exp(-W_k)$ for the shell to be the same as for the corresponding core. This may seem contrary to the previous work but is a negligible approximation here because the Debye–Waller term is fairly close to unity for the values of $\sin\theta/\lambda$ at which any effect is significant.

The problem in evaluating (2) is to obtain an estimate for the shell scattering factor $f_{sk}(K)$. It is important to use the number of electrons in the shell [here represented as $Y(k)$] that the model constants imply, because the shell model is parameterized to represent the dipole moment $\mathbf{p}(k/\mathbf{q}j)$ in the phonon mode, where

$$\mathbf{p}(k/\mathbf{q}j) = -Y(k)e\mathscr{W}(k/\mathbf{q}j), \quad (3)$$

and is not fitted individually for charge or displacement. The shell model is therefore not based on any specific identification of the shell electrons with a particular subset of the entire electronic configuration. (Indeed one can vary the number of electrons in the shell while maintaining constant core vibrational frequencies *and* polarization vectors.) Hence it is inappropriate to search for some underlying exact representation of the shell scattering factor from purely lattice dynamical arguments. This is just as well because one is not readily available. For example, in the tetragonally bonded zinc-blende-structure compounds that provide the numerical basis of this study, the valence electrons that one would naturally associate with the shell are certainly not described by a superposition of atomic ground-state wavefunctions. Fortunately, any reasonable decay of $f_{sk}(K)$ with scattering vector will give a useful estimate of the

shell contribution to the scattering, due to the scaling imposed by (3) and the necessary limit at zero $\sin\theta/\lambda$ that

$$f_{sk}(0) = Y(k). \quad (4)$$

One result of Dawson's (1964) discussion of sp^3 hybrid-orbital scattering factors of relevance to the zinc-blende-structure materials was to show that a spherically averaged scattering factor could be derived to a good approximation from the partial scattering factor for (s) electrons. *International Tables for X-ray Crystallography* (1974) gives the $\sin\theta/\lambda$ dependence of these scattering factors for $2s$, $3s$ and $4s$ electrons for various atoms. For the $3s$ and $4s$ atoms listed, they fall from $1 \cdot 0$ per electron at much the same rate, typically decaying to $0 \cdot 5$ by $\sin\theta/\lambda$ about $0 \cdot 15 \text{Å}^{-1}$. Guided by Matthew & Yousif's (1984) discussion (in a related context), $f_{sk}(K)$ was parameterized by the hydrogenic function:

$$f_{sk}(K) = Y(k)\left(1+\frac{K^2a^2}{12Z^2}\right)\Big/\left(1+\frac{K^2a^2}{4Z^2}\right)^4 \quad (5)$$

with the hydrogenic charge parameter Z chosen as $1 \cdot 1$, to give the fall in $f_{sk}(K)$ to $Y(k)/2$ at $\sin\theta/\lambda = 0 \cdot 15 \text{Å}^{-1}$. a is the Bohr radius. This expression was used for all models, including those valence-shell models that showed an unphysical negative $Y(k)$. This preserves the dipole moments produced by the models which, as can be seen from (2), (3) and (5), are the ultimate source of the effect.

In summary, the general features of the results of the next section are not sensitive to the particular choice of shell scattering factor. For this study there is no point in distinguishing small features in the valence scattering factor and, in view of the modest size of the whole effect, these are likely to be difficult to see experimentally.

Results

Table 1 shows the shell charges for shell models relevant to the 14 zinc-blende-structure materials discussed by Reid (1983b) and to the group IV elements. These charges are used in (5) along with the corresponding shell–core displacements of the models. With the subroutines of Kunc & Nielsen (1979), eigendata were generated to evaluate (1) and (2) and hence the percentage effect, P, of shell scattering processes, where

$$P = 100[I_s(\mathbf{K}) - I(\mathbf{K})]/I(\mathbf{K}). \quad (6)$$

Atomic scattering factors were taken in the parameterized form given in *International Tables for X-ray Crystallography* (1974) and anomalous-dispersion corrections were included for Mo $K\alpha$ radiation. Shell scattering factors were calculated as discussed in the previous section (without anomalous dispersion).
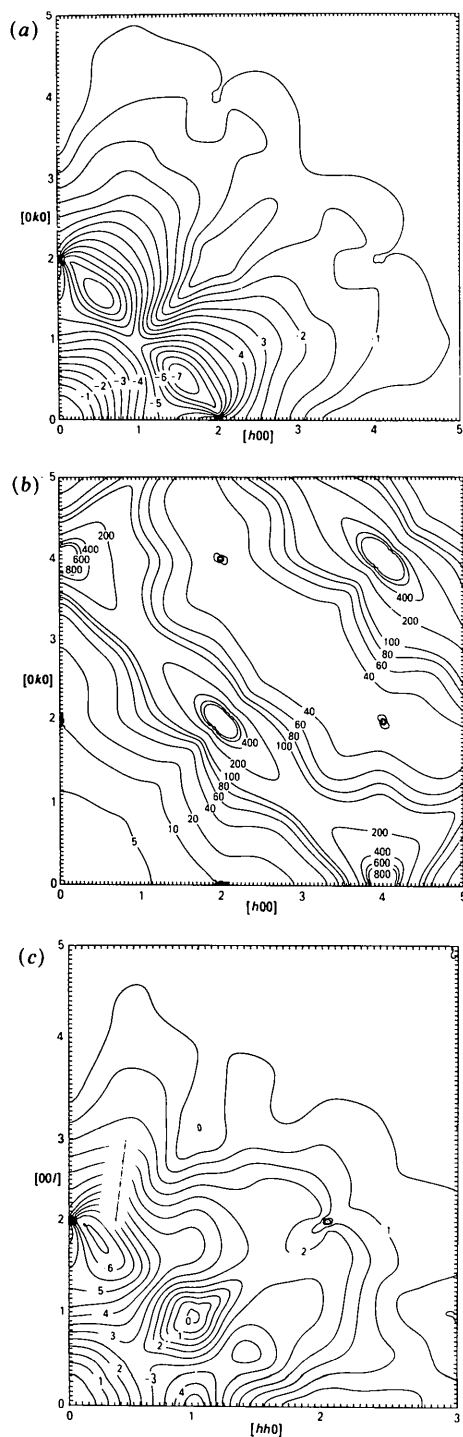
Fig. 1. (a) Contours of the shell scattering, P of equation (5), in steps of -0.5% given by the shell model for GaAs in the (001) plane at 295K. The zero values at 200 and 020 produce somewhat larger contour distortions than should be present because the sampled data spacing increments q coordinates by 0.05 $(2\pi/d)$ whereas P falls noticeably to zero only when $q < 0.03$ $(2\pi/d)$. (b) One-phonon contours in electron units per cell over the same area with contour levels 5, 10, 20, 40, 60, 80, 100, 200, 400, 600 and 800. Contours close to Bragg reflections show small irregularities due to the contouring algorithm. (c) As for (a) but in the ($1\bar{1}0$) plane.

Table 1. *Shell charges in units of $-e$ for cation $Y(1)$ and anion $Y(2)$ derived from the shell models listed for* 14 *zinc-blende-structure materials and the four group IV elements*

SM signifies 'shell model' and VSM 'valence shell model'. Full references to the zinc-blende-material models, including some corrections to published parameters, are given by Reid (1983*a*). The group IV element models are summarized by Price, Rowe & Nicklow (1971) except that for diamond the quoted δ_R was divided by 4 to produce the correct frequencies.

Material	Model	Shell charges	
		$Y(1)$	$Y(2)$
GaP	SM	1·571	1·863
	VSM	−6·03	1·87
GaAs	SM	1·565	3·73
	VSM	−7·12	2·51
GaSb	SM*A*	6·251	6·039
	SM*B*	5·490	6·329
	VSM	−5·71	2·83
InP	VSM	−6·13	1·64
InAs	VSM*A*	−5·80	2·39
	VSM*B*	−7·12	2·51
InSb	SM	4·022	6·081
	VSM	−5·48	3·15
ZnO	VSM	−7·44	1·68
ZnS	VSMI*a*	6·13	5·61
	VSMII*a*	−6·77	2·06
ZnSe	VSM	−6·62	2·50
ZnTe	VSMI	1·63	5·37
	VSMII	−5·12	2·24
CdTe	SMI	1·680	5·447
	SMII	2·487	5·98
CuCl	SM	0·070	0·626
CuBr	SMI	14·873	1·884
	SMII	1·334	1·078
CuI	SM	0·140	60·120
C	SM	3·801	3·801
Si	SM	2·866	2·866
Ge	SM	2·526	2·526
α-Sn	SM	6·200	6·200

Fig. 1(*a*) shows contours for P in one quadrant of the (001) plane as given by the shell model of Dolling & Waugh (1965) for GaAs at room temperature. P tends to zero at Bragg reflections because $W(k/qj) \to 0$ as $q \to 0$ for the acoustic modes. It is only exactly zero at the reciprocal-lattice point itself and it is found, *e.g.* around 200, that it may become appreciable for q values of only 0.01 $(2\pi/d)$. The effect rises to its greatest values in off-symmetry directions, peaking at about -7%. The overall structure should be accessible to experimental verification, though it is clear from the contours of $I(\mathbf{K})$ over the same area, shown in Fig. 1(*b*), that the shell contribution is most pronounced in a region where the one-phonon scattering is weaker than average. Fig. 1(*c*) illustrates that the percentage P tends to be smaller in the ($1\bar{1}0$) plane.

Shell models calculated for GaP, GaSb, InSb and CdTe as a sample of other materials showed similar patterns of negative percentage effect, *i.e.* the inclusion of shell processes reduced the total X-ray scattering. The maximum values were respectively -5.2, -3.7, -4.3 and -2.4%. In general, the valence-shell models showed an effect of significantly different structure and size from that shown by the shell
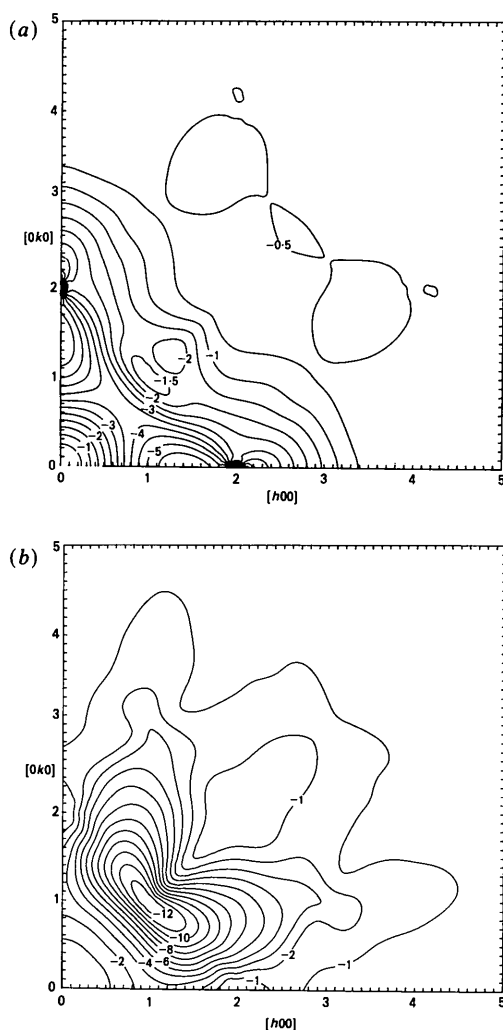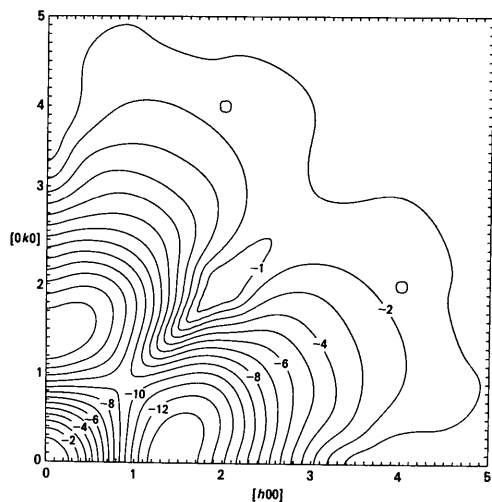
models. Fig. 2(a) shows contours of P in one quadrant of the (001) plane for the valence-shell model of GaAs and Fig. 2(b) the valence-shell model Ia for ZnS. Fig. 3 shows an even larger effect for the light atoms of silicon and illustrates the minor point that the effect does not go to zero at forbidden reflections (such as 200 in silicon).

The general theoretical conclusion may be drawn that deforming atoms cause a moderate but significant change in the one-phonon scattering, the amount depending on the representation of the ionic deformation and the lattice dynamical model. Although lighter and more polarizable ions are more significant, if the models presented here are a useful guide, the effect should be quite demonstrable in the III-V semiconductors.

The deformation should be experimentally accessible if the harmonic one-phonon scattering can be isolated. The effect has the distinct advantage that it occurs in a region of reciprocal space where the scattering is free from anharmonic effects and largely free from multiphonon scattering (Reid, 1983a). The most obvious approach to detection and measurement is to perform a classic absolute scattering experiment from extended-face single crystals [as described for instance by Schuster & Weymouth (1971)], scanning the scattering vector K over an appropriate region. After subtraction of the best estimate of the Compton scattering and phonon scattering, the residual scattering will contain the deformation effect. It will also contain the diffuse scattering due to any other perturbing effect, which makes it important that the structure of the residue over an extended region is examined, rather than confining detection to a few spot measurements. A program of experimental diffuse scattering measurements relevant to this problem is under way.

Fig. 2. (a) GaAs as in Fig. 1(a), showing the prediction of the valence-shell model. (b) ZnS over the same area, as given by the valence-shell model Ia. Contour spacing −1%.

APPENDIX

The notation for the scattering cross section is as follows:

$I(K)/N\sigma_0 I_0$ cross section in electron units per cell
K scattering vector
q phonon wavevector
j phonon branch number
E average energy in mode (qj) at temperature T.
$$E(qj) = \hbar\omega(qj)$$
$$\times (1/\{\exp[\hbar\omega(qj)/k_BT]-1\}+\tfrac{1}{2}),$$
where k_B is Boltzmann's constant
$\omega(qj)$ angular frequency associated with mode (qj)
k labels ions within primitive unit cell

Fig. 3. Contours of the percentage contribution of the shell scattering, P of equation (5), in steps of −1%, given by the shell model for silicon in the (001) plane at 295K.

$f_k(K)$	complex scattering factor of whole of kth ion
$f_{sk}(K)$	scattering factor of shell of kth ion
$-W_k$	Debye–Waller exponent $= -B_k \sin^2 \theta / \lambda^2$
$\mathscr{E}(k/\mathbf{q}j)$	orthonormalized eigenvector for ion k in mode $(\mathbf{q}j)$
$\mathscr{W}(k/\mathbf{q}j)$	relative shell–core displacement eigenvector for ion k in mode $(\mathbf{q}j)$
G	a reciprocal-lattice vector
$\mathbf{r}(k)$	equilibrium position of kth ion relative to origin of unit cell.

References

BORN, M. (1942). *Rep. Prog. Phys.* **9**, 294–333.
COCHRAN, W. & COWLEY, R. A. (1967). *Handbuch der Physik* XXV/29, pp. 59–156. Berlin: Springer.

DAWSON, B. (1964). *Acta Cryst.* **17**, 997–1009.
DOLLING, G. & WAUGH, J. L. T. (1965). *Lattice Dynamics*, edited by R. F. WALLIS, pp 19–32. Oxford: Pergamon.
International Tables for X-ray Crystallography (1974). Vol. IV. Birmingham: Kynoch Press. (Present distributor D. Reidel, Dordrecht.)
KUNC, K. & NIELSEN, O. H. (1979). *Comput. Phys. Commun.* **17**, 413–422.
MARCH, N. H. & WILKINS, S. W. (1978). *Acta Cryst.* **A34**, 19–26.
MATTHEW, J. A. D. & YOUSIF, S. Y. (1984). *Acta Cryst.* **A40**, 716–721.
MELVIN, J. S., PIRIE, J. D. & SMITH, T. (1968). *Phys. Rev.* **175**, 1082–1090.
PRICE, D. L., ROWE, J. M. & NICKLOW, R. M. (1971). *Phys. Rev. B*, **3**, 1268–1279.
REID, J. S. (1974). *Phys. Status Solidi B*, **64**, 57–64.
REID, J. S. (1983a). *Acta Cryst.* **A39**, 1–13.
REID, J. S. (1983b). *Acta Cryst.* **A39**, 533–538.
SCHUSTER, S. L. & WEYMOUTH J. W. (1971). *Phys. Rev. B*, **3**, 4143–4153.

Problems Associated with the Measurement of X-ray Attenuation Coefficients. I. Silicon

Report on the International Union of Crystallography X-ray Attenuation Project

By D. C. CREAGH*

Physics Department, Royal Military College, Duntroon, ACT 2600, Australia

AND J. H. HUBBELL

Center for Radiation Research, National Bureau of Standards, Gaithersburg, MD 20899, USA

Abstract

X-ray attenuation coefficient measurements made on single-crystal silicon specimens by participants in the International Union of Crystallography X-ray Attenuation Project are presented for the energy range 8–60 keV. Twelve laboratories using eight different experimental configurations have provided data for analysis. A comparison is made between measurements using the different techniques at those characteristic wavelengths of interest to crystallographers. Comparison of these measurements with available theoretical cross sections suggests that a model in which the thermal diffuse scattering cross section is used instead of the Rayleigh scattering cross section for the calculation of the theoretical total scattering cross section gives better agreement with the experimental values. No basis was found for preferring one of three current theoretical tabulations of photoelectric absorption cross section over the others.

* Present address: Physics Department, University College, Australian Defence Force, Campbell, ACT 2600, Australia.

1. Introduction

1.1. *Tables of X-ray attenuation coefficients*

Following the discovery by Röntgen (1895) of the penetrating nature of X-rays, a considerable body of numerical data concerning the attenuation of X-rays by matter has accumulated in the scientific literature. The earliest quantitative measurements of X-ray attenuation coefficients appear to be those by Barkla & Sadler (1907), after which researchers in a wide variety of disciplines (*e.g.* X-ray crystallography, atomic physics, medical diagnosis and therapy, electron probe microanalysis) contributed data sets which form the basis of such widely circulated compilations as those by McMaster, Del Grande, Mallett & Hubbell (1969) and by Storm & Israel (1970). The McMaster *et al.* (1969) compilation includes a list of data sources and a confidence weight assigned to each data-source document. A data index to these data sources through 1971 was given by Hubbell (1971).

Many other compilations exist [*e.g.* Allen (1935, 1969); Victoreen (1949); Liebhafsky, Pfeiffer, Win-